

An introduction to Plasma Tomography

Diogo R. Ferreira*

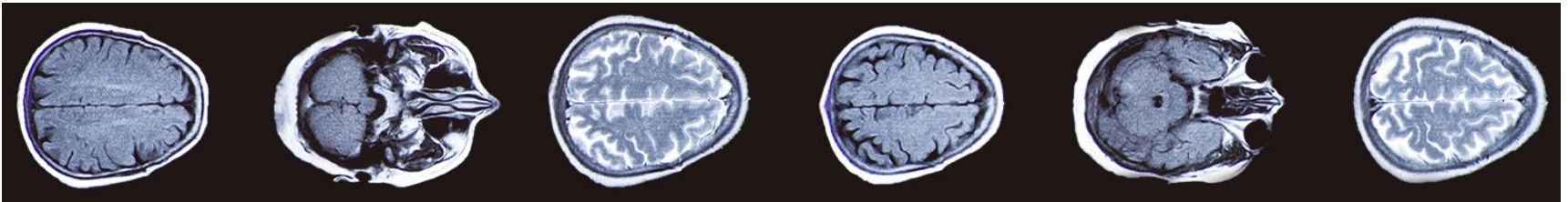
IPFN/IST, University of Lisbon

diogo.ferreira@tecnico.ulisboa.pt

(*special thanks to: Daniel H. Costa, Diogo D. Carvalho, Pedro J. Carvalho, André S. Duarte, Hugo Alves, Luís Guimarães, Horácio Fernandes, José M. Bioucas-Dias)

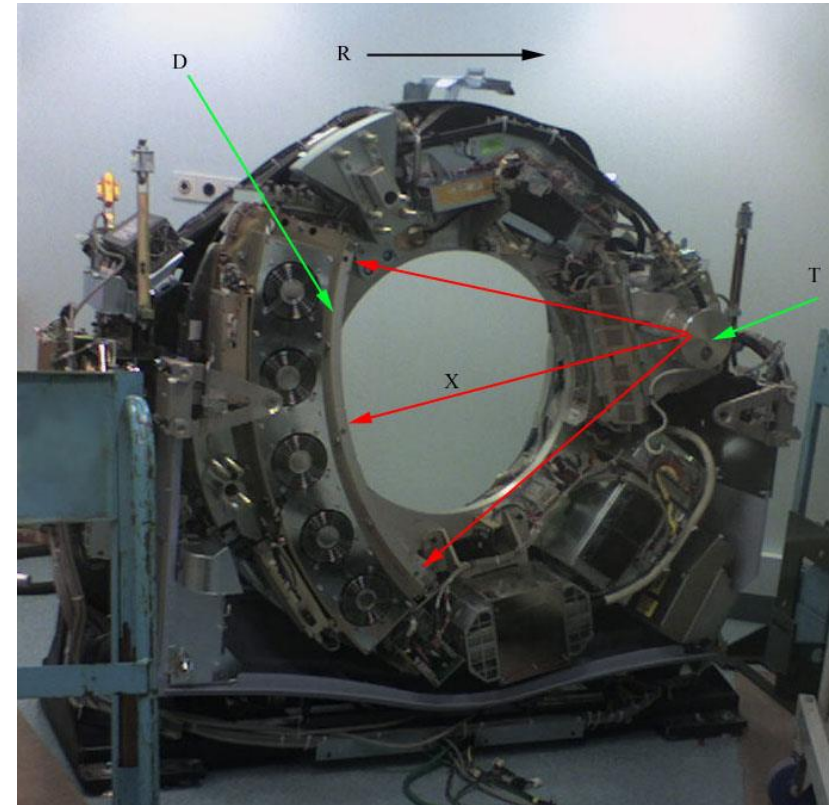
Computed Tomography

- Medical applications



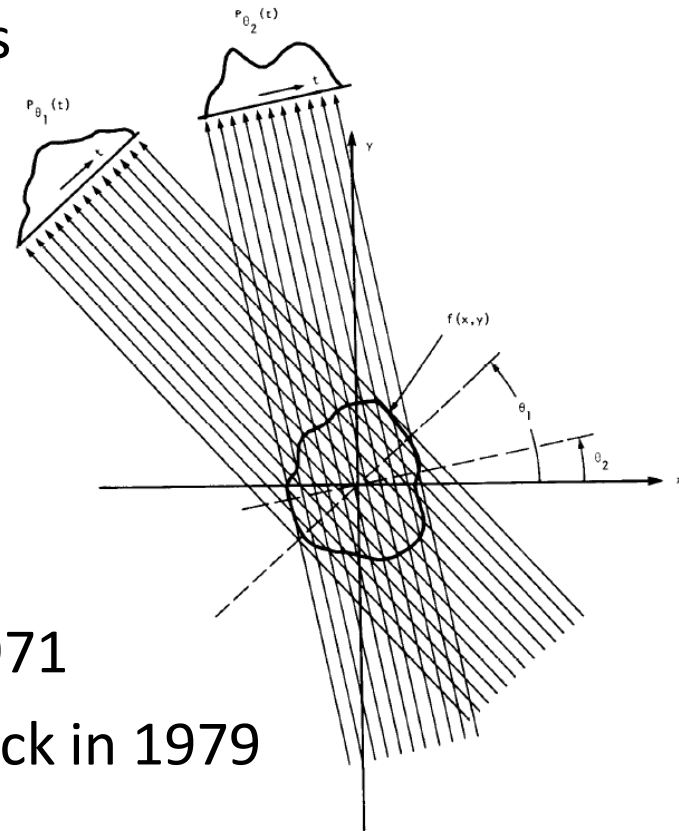
Computed Tomography

- CT scanner internals



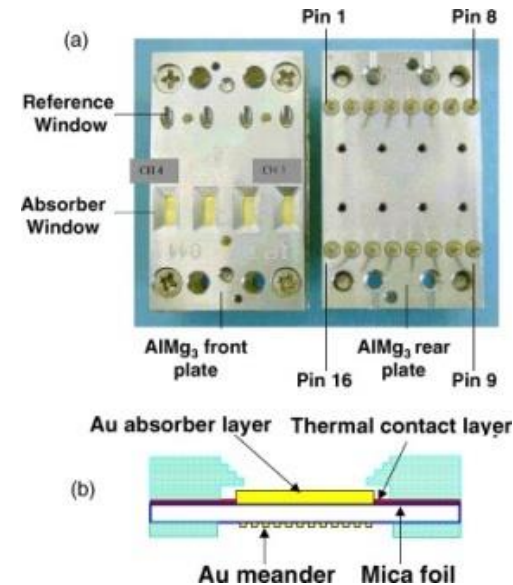
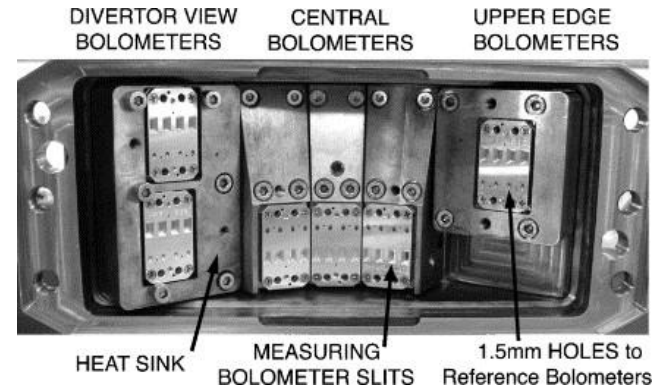
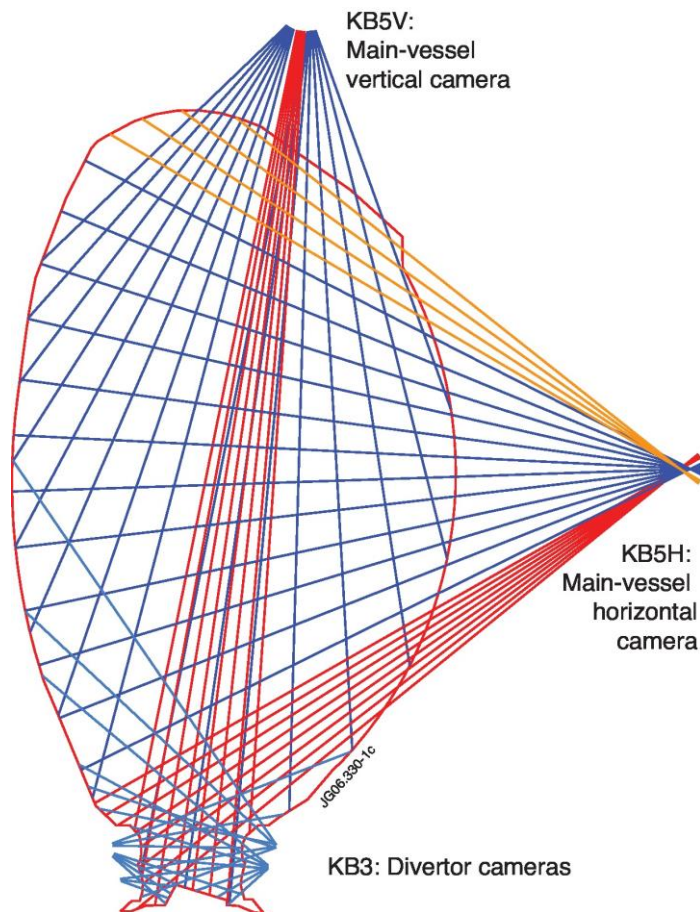
Computed Tomography

- Tomography problem
 - reconstruct image from its projections
 - each projection at a different angle
 - integral of the image at that angle
 - paper by J. Radon in 1917
 - Radon transform
 - inverse Radon transform
 - algorithm by A. Cormack in 1963-64
 - first CT scanner by G. Hounsfield in 1971
 - Nobel prize for Hounsfield and Cormack in 1979



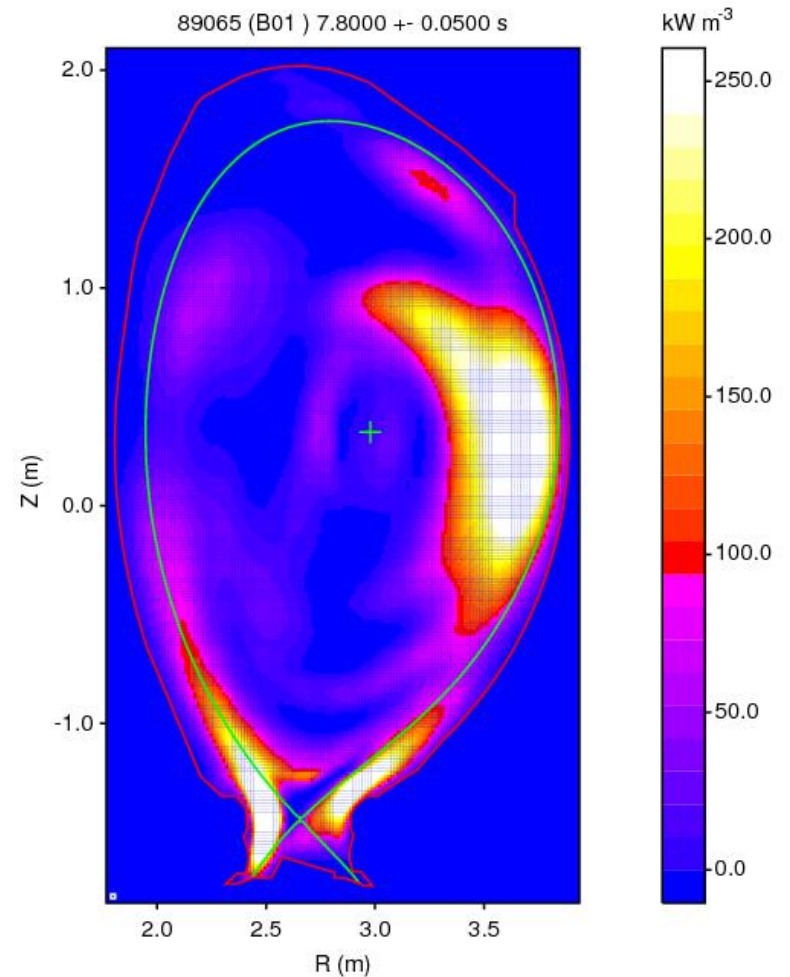
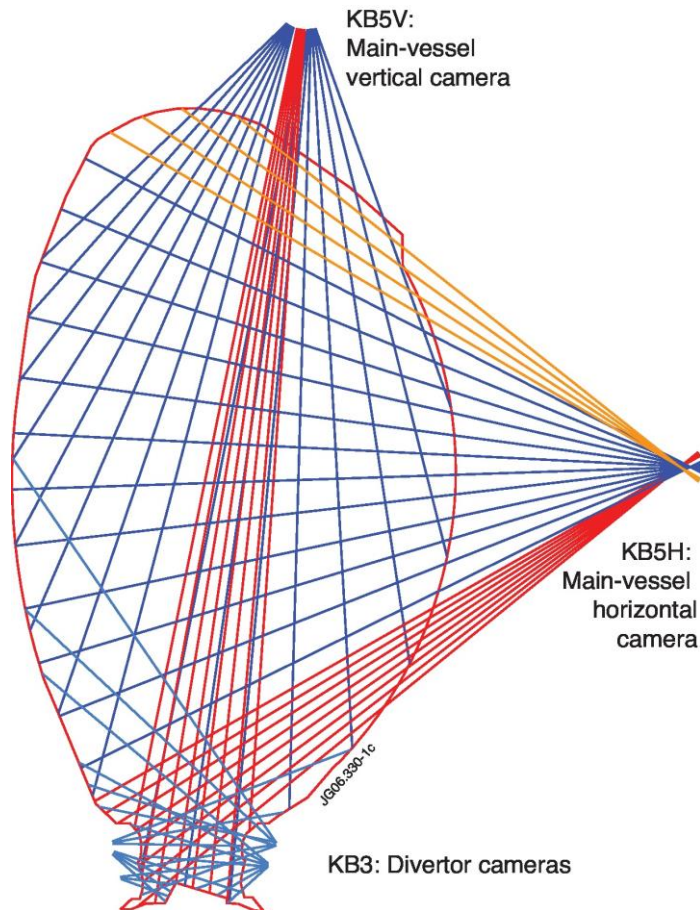
Plasma Tomography

- Tomography at the Joint European Torus (JET)



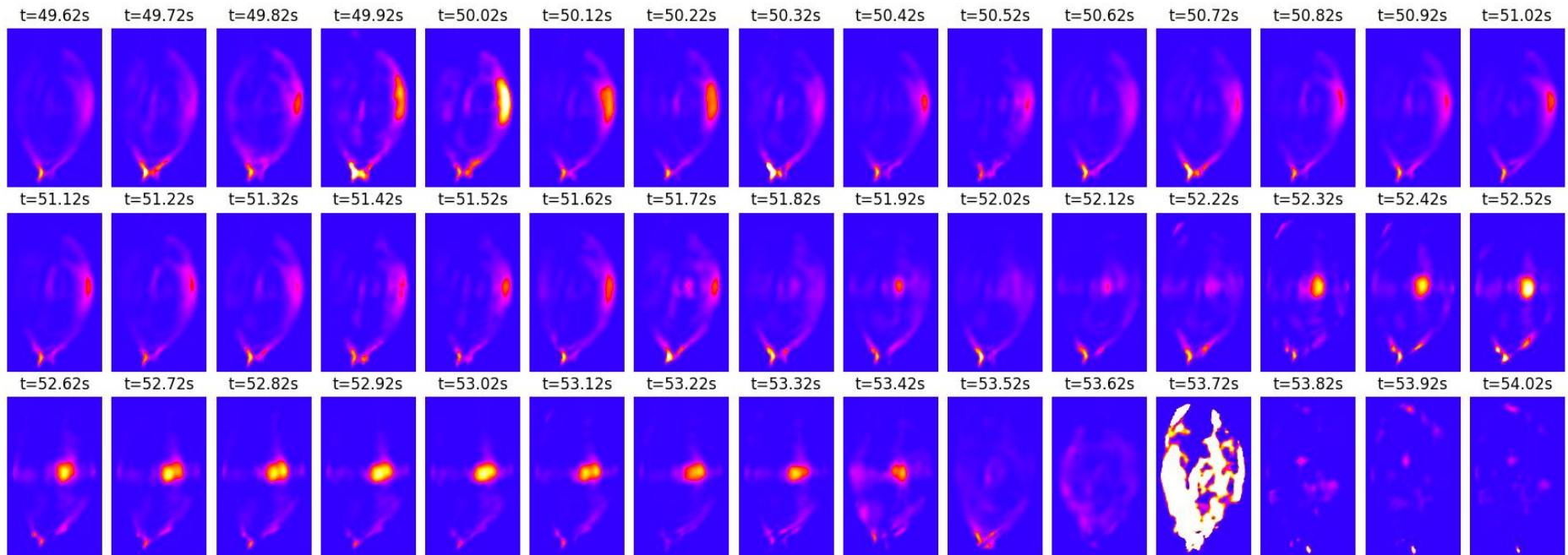
Plasma Tomography

- Tomography at the Joint European Torus (JET)



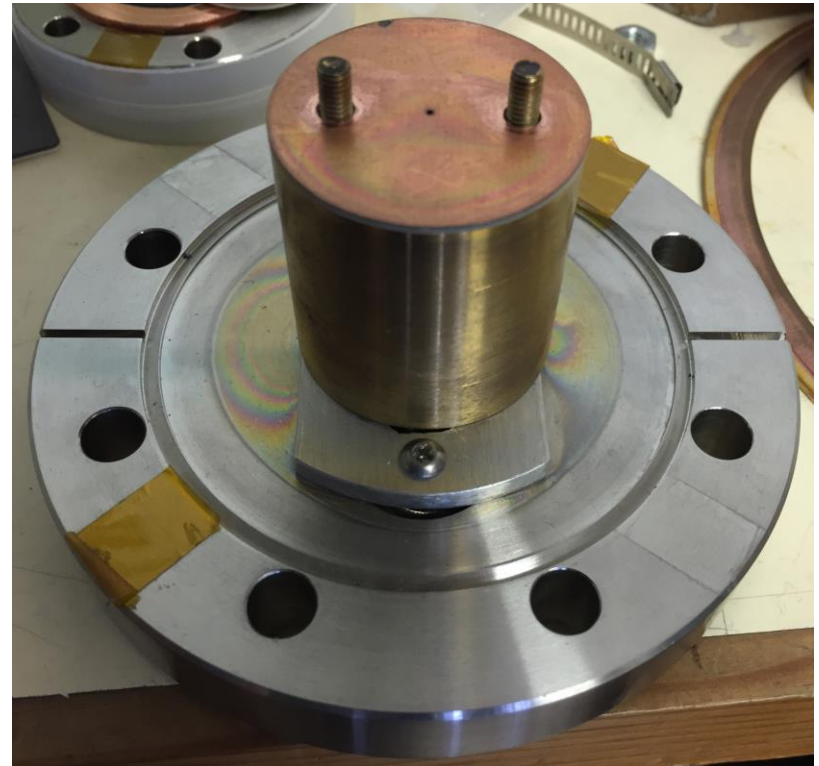
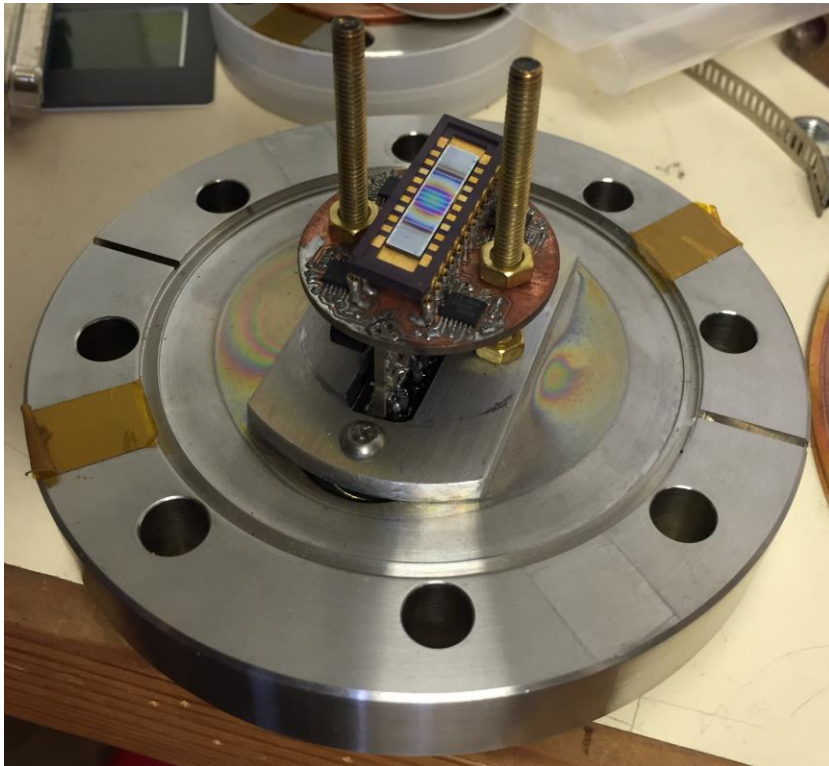
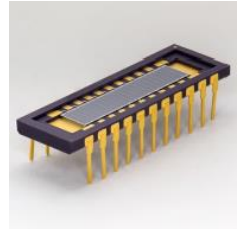
Plasma Tomography

- Tomography at the Joint European Torus (JET)

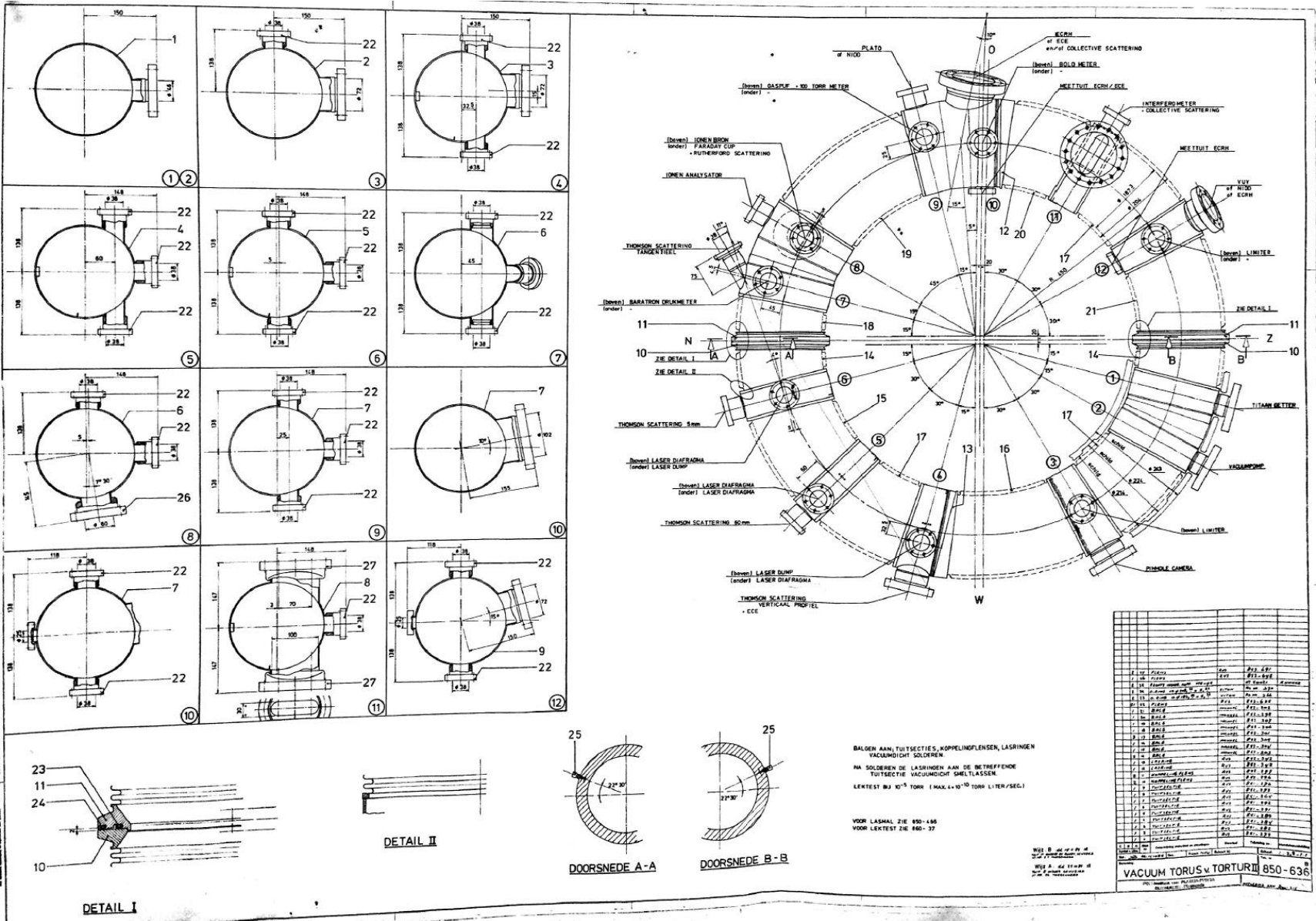


Plasma Tomography

- Tomography at ISTTOK
 - cameras based on photodiode array + pinhole

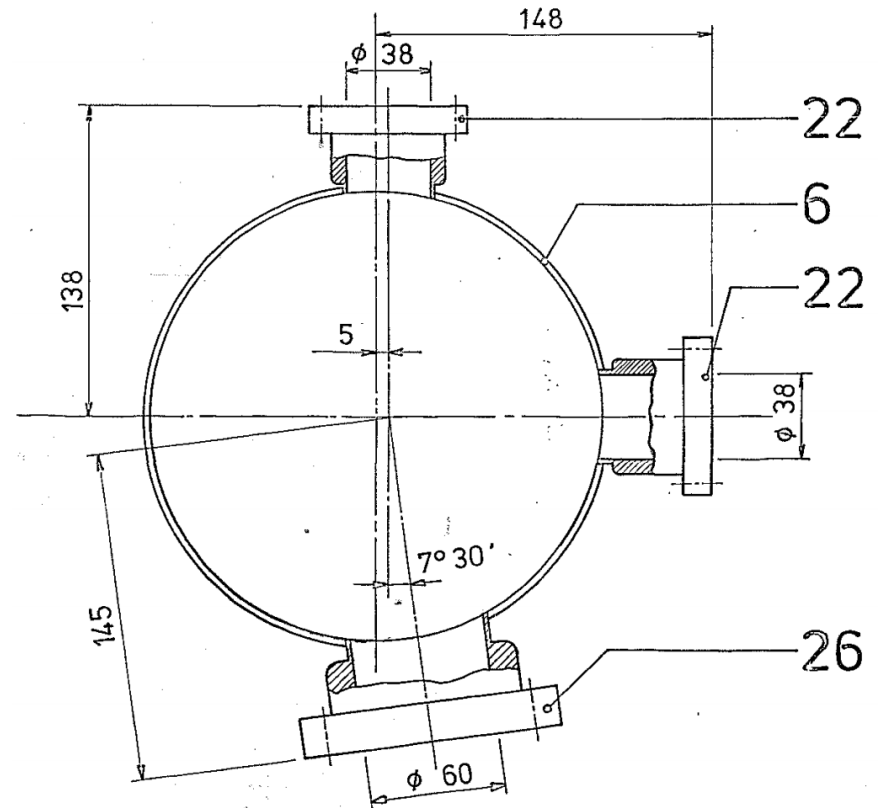


Plasma Tomography



Plasma Tomography

- ISTTOK setup (2019)
 - 2 cameras
 - vertical, horizontal
 - 16 detectors per camera
 - in fact 20 detectors, but 4 are not used
 - lines of sight can be derived from detector and pinhole positions

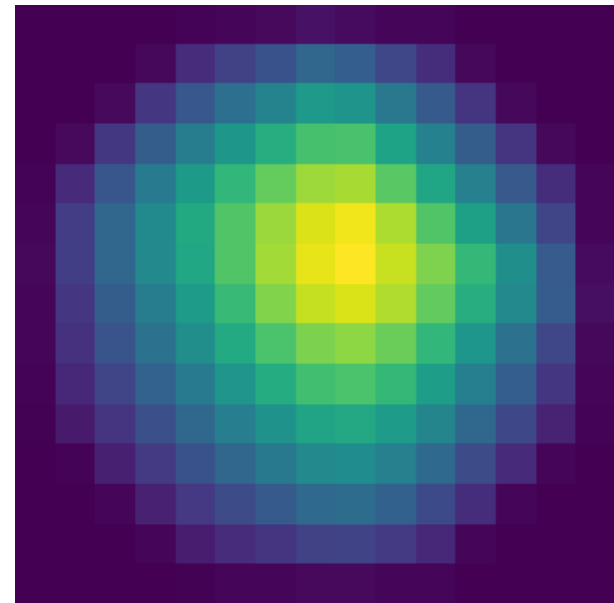
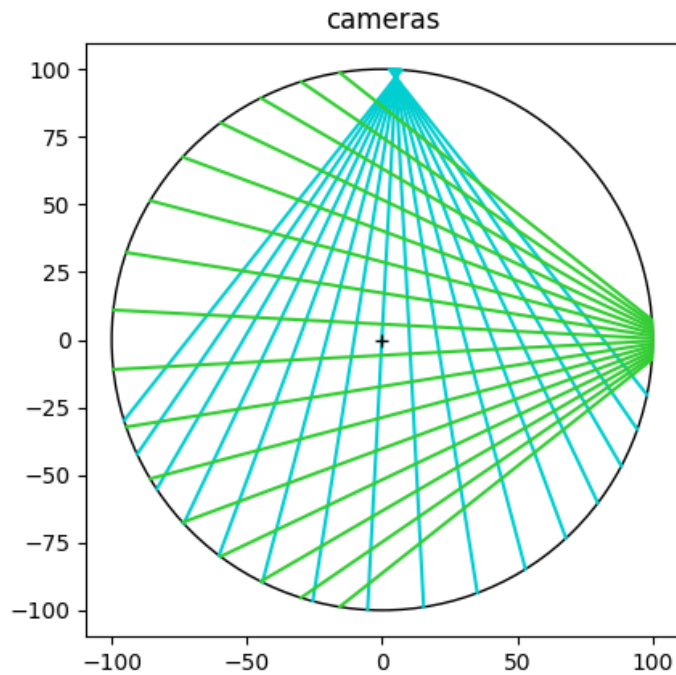


Plasma Tomography

- Tomography methods
 - analytical methods (Fourier-based)
 - Fourier slice theorem
 - filtered backprojection (FBP)
 - Cormack's approach with basis functions
 - algebraic methods (pixel-based)
 - system of linear equations
 - iterative reconstruction techniques such as ART
 - solutions using regularization

Plasma Tomography

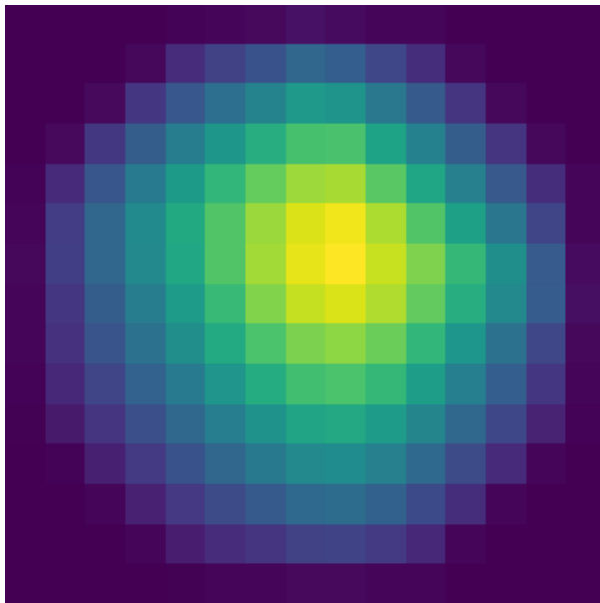
- Inverse problem
 - from detector measurements to plasma profile



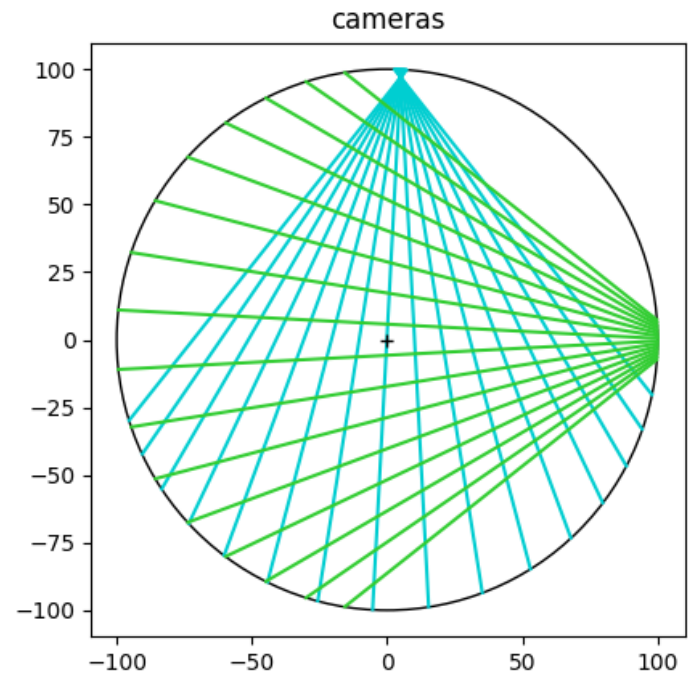
15x15 resolution

Plasma Tomography

- Forward problem
 - from plasma profile to detector measurements

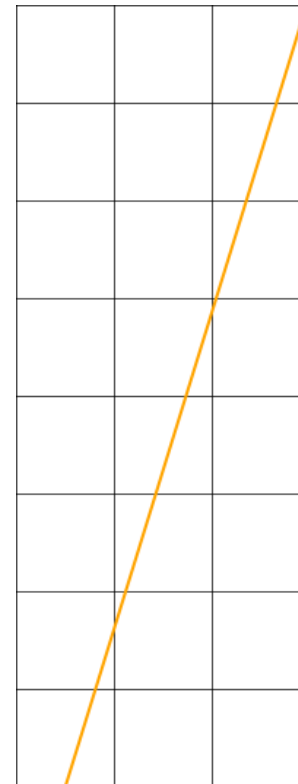
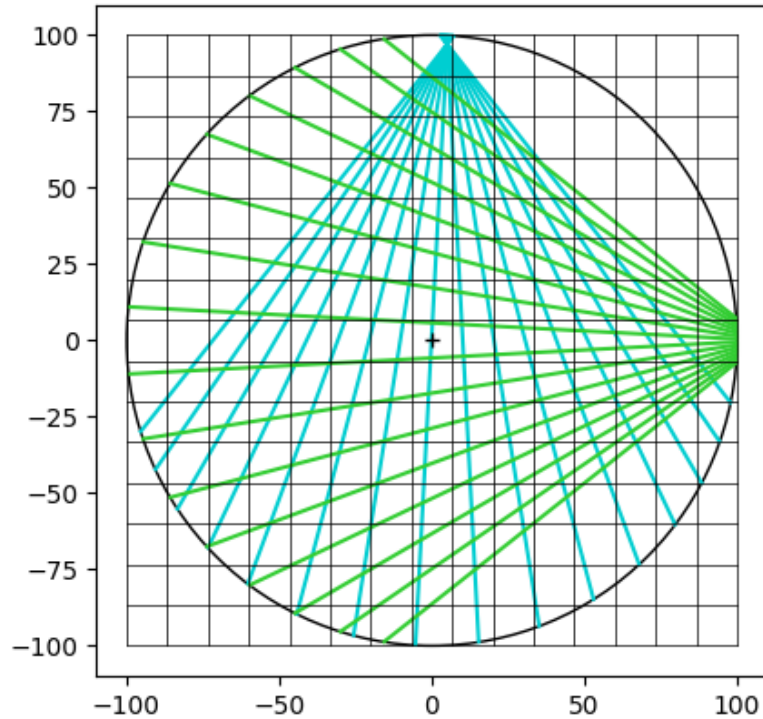


15x15 resolution



Plasma Tomography

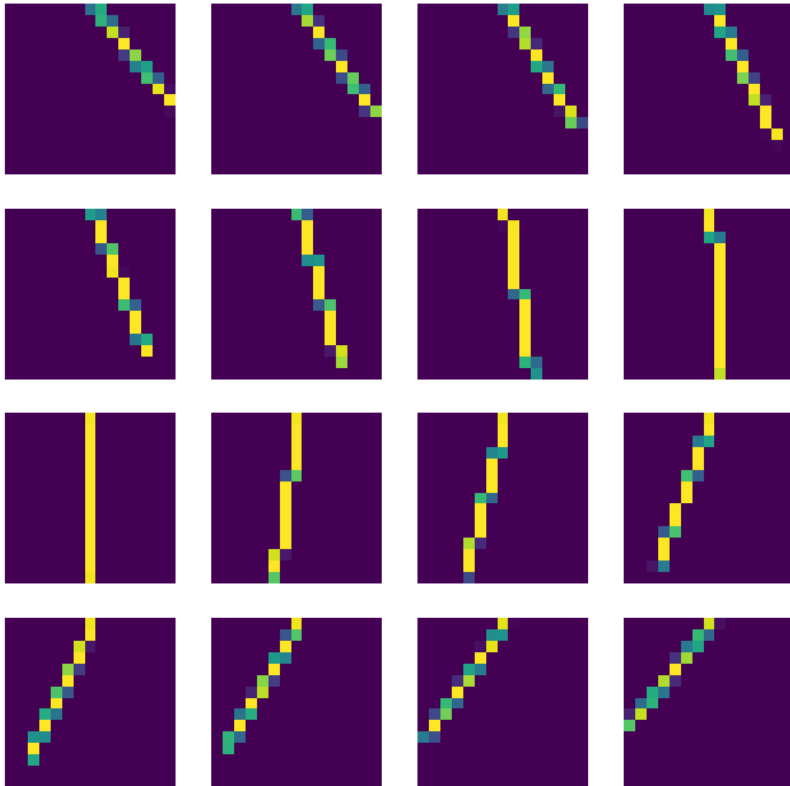
- Geometry of the problem
 - find the contribution of each pixel for each line of sight



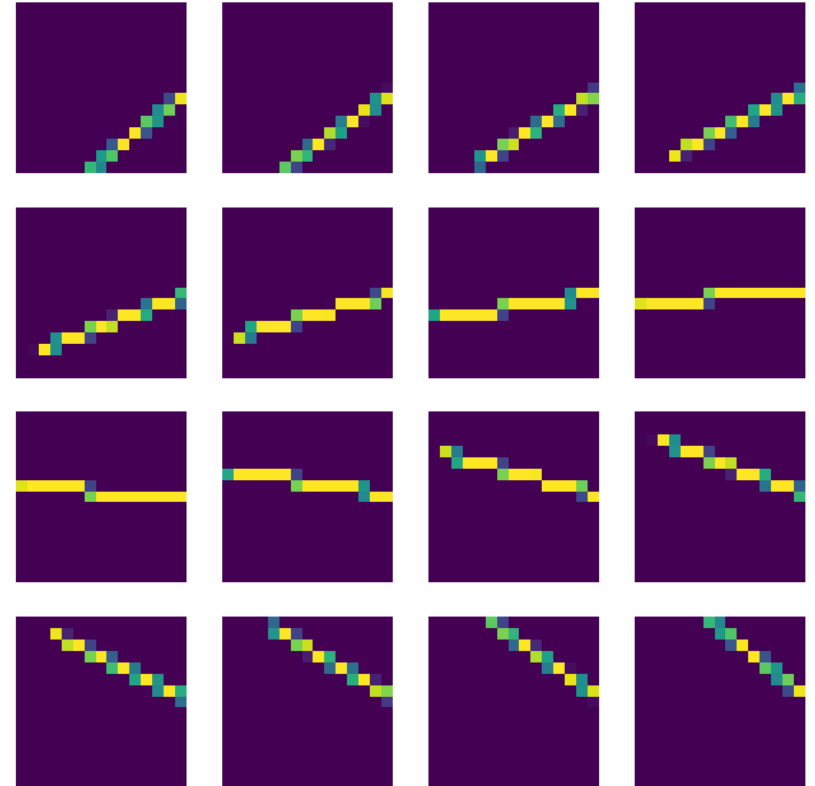
Plasma Tomography

- Contribution of each pixel to each line of sight

projections (vertical camera)

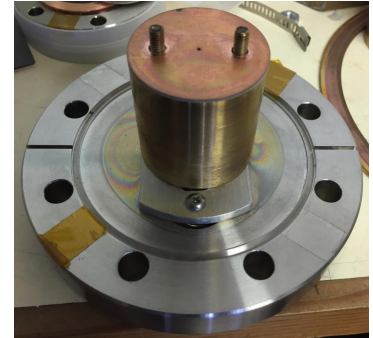
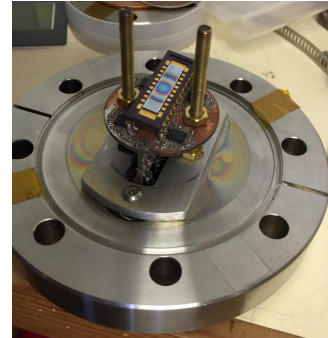
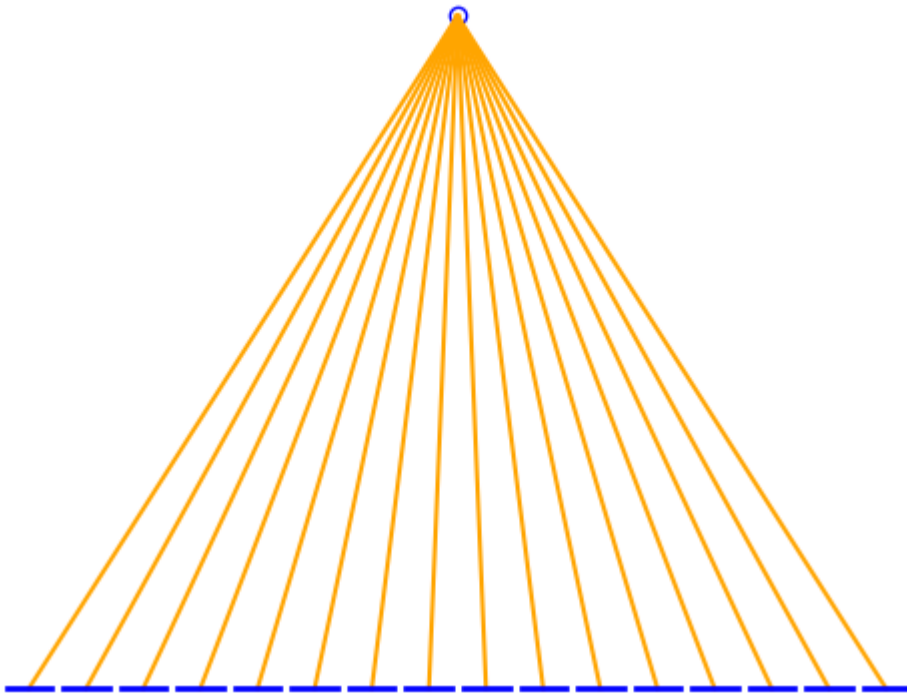


projections (horizontal camera)



Plasma Tomography

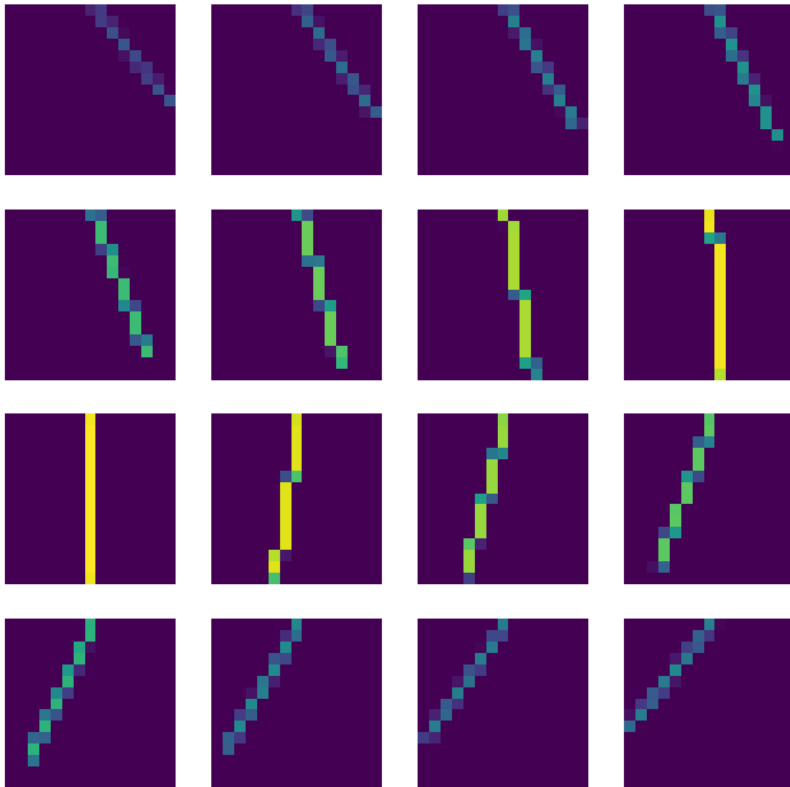
- Calibration factors (*étendue*)
 - angle of incidence on the detector
 - angle through the pinhole (and thickness)



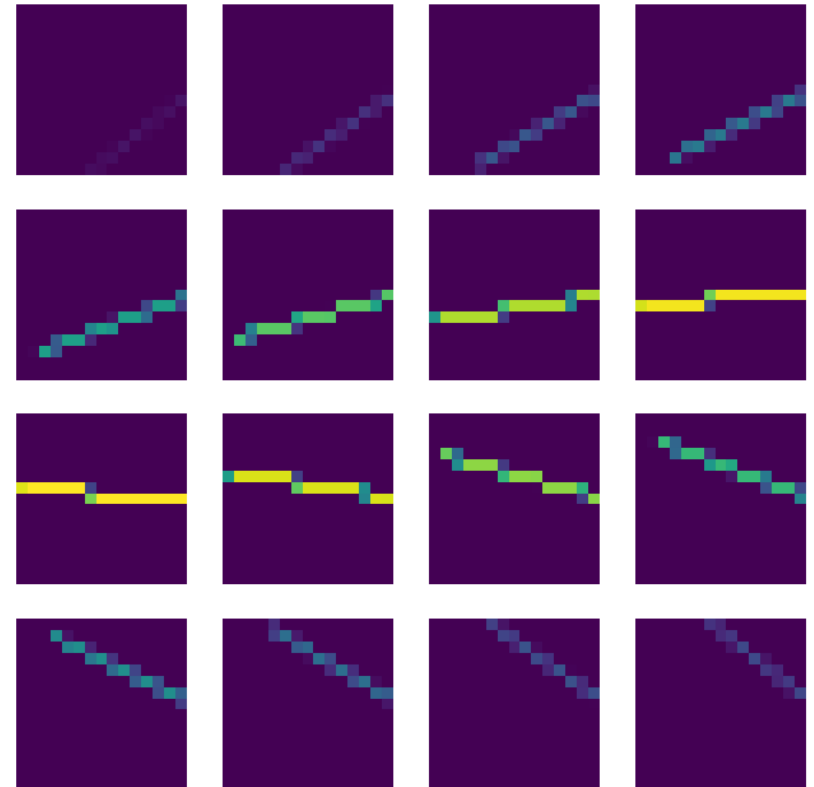
Plasma Tomography

- Contribution of each pixel to each line of sight

projections (vertical camera)

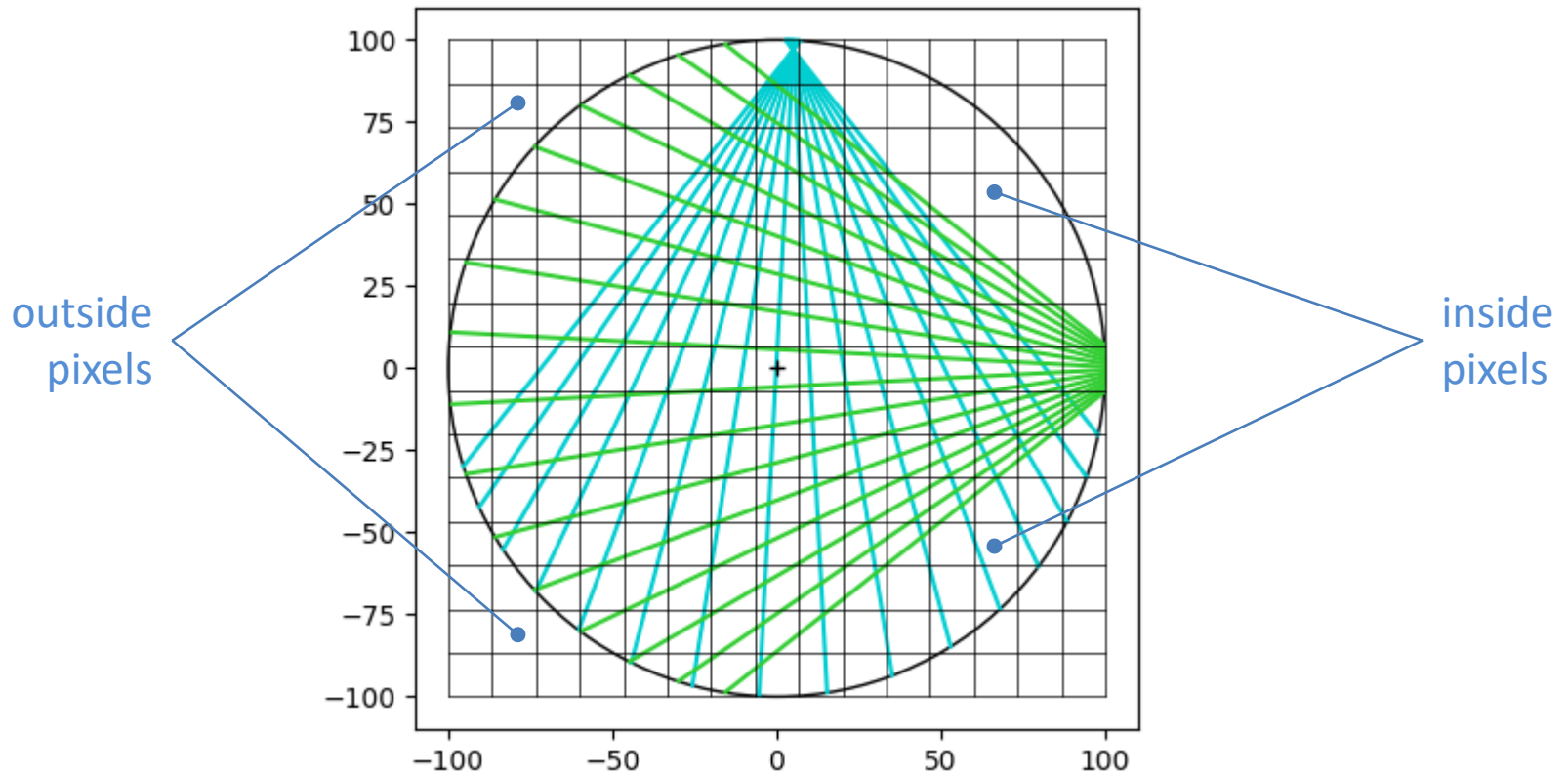


projections (horizontal camera)



Plasma Tomography

- Underdetermined system



Plasma Tomography

- Regularization (general)
 - minimize:

$$\phi = \|\mathbf{f} - \mathbf{P}\mathbf{g}\|^2 + \alpha\|\mathbf{R}\mathbf{g}\|^2$$

$$\frac{\partial \phi}{\partial \mathbf{g}} = 0 \Rightarrow \mathbf{g} = (\mathbf{P}^T \mathbf{P} + \alpha \mathbf{R}^T \mathbf{R})^{-1} \mathbf{P}^T \mathbf{f}$$

$$\mathbf{g} = (\mathbf{P}^T \mathbf{P} + \alpha_1 \mathbf{R}_1^T \mathbf{R}_1 + \alpha_2 \mathbf{R}_2^T \mathbf{R}_2 + \dots)^{-1} \mathbf{P}^T \mathbf{f}$$

Plasma Tomography

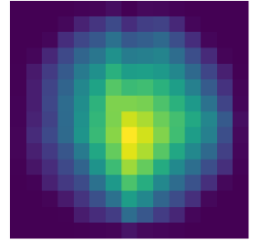
- Regularization (simple approach)
 - for every pixel
 - minimize the horizontal and vertical differences to neighbors
 - for outside pixels
 - minimize their norm

$$\phi = \|\mathbf{f} - \mathbf{P}\mathbf{g}\|^2 + \alpha_1 \|\mathbf{D}_h \mathbf{g}\|^2 + \alpha_2 \|\mathbf{D}_v \mathbf{g}\|^2 + \alpha_3 \|\mathbf{I}_o \mathbf{g}\|^2$$

$$\mathbf{g} = (\mathbf{P}^T \mathbf{P} + \alpha_1 \mathbf{D}_h^T \mathbf{D}_h + \alpha_2 \mathbf{D}_v^T \mathbf{D}_v + \alpha_3 \mathbf{I}_o^T \mathbf{I}_o)^{-1} \mathbf{P}^T \mathbf{f}$$

Plasma Tomography

- Regularization matrix \mathbf{D}_h



$$225 \times 225 \begin{bmatrix} 1 & -1 & 0 & 0 & 0 & \dots & 0 & 0 \\ 0 & 1 & -1 & 0 & 0 & & 0 & 0 \\ 0 & 0 & 1 & -1 & 0 & & 0 & 0 \\ 0 & 0 & 0 & 1 & -1 & & 0 & 0 \\ 0 & 0 & 0 & 0 & 1 & & 0 & 0 \\ \vdots & & & & & \ddots & & \vdots \\ 0 & 0 & 0 & 0 & 0 & & -1 & 0 \\ 0 & 0 & 0 & 0 & 0 & & 1 & -1 \\ -1 & 0 & 0 & 0 & 0 & \dots & 0 & 1 \end{bmatrix}$$

Plasma Tomography

- Regularization matrix \mathbf{D}_V

15 pixels
 • Regularization matrix \mathbf{D}_V

15 pixels

$$\begin{bmatrix} 1 & 0 & 0 & 0 & 0 & 0 & 0 & 0 & 0 & 0 & 0 & 0 & 0 & 0 & 0 & -1 & 0 & 0 & \dots & 0 \\ 0 & 1 & 0 & 0 & 0 & 0 & 0 & 0 & 0 & 0 & 0 & 0 & 0 & 0 & 0 & 0 & -1 & 0 & & 0 \\ 0 & 0 & 1 & 0 & 0 & 0 & 0 & 0 & 0 & 0 & 0 & 0 & 0 & 0 & 0 & 0 & 0 & -1 & & 0 \\ \vdots & & & & & & & & & & & & & & & & & & \ddots & \vdots \\ 0 & 0 & 0 & 0 & 0 & 0 & 0 & 0 & 0 & 0 & 0 & 0 & -1 & 0 & 0 & 0 & 0 & 0 & & 0 \\ 0 & 0 & 0 & 0 & 0 & 0 & 0 & 0 & 0 & 0 & 0 & 0 & 0 & -1 & 0 & 0 & 0 & 0 & \dots & 0 \\ 0 & 0 & 0 & 0 & 0 & 0 & 0 & 0 & 0 & 0 & 0 & 0 & 0 & 0 & -1 & 0 & 0 & 0 & & 1 \end{bmatrix}$$

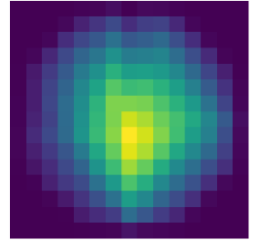
225x225

Plasma Tomography

- Regularization matrix \mathbf{I}_0

225x225

$$\begin{bmatrix} 1 & 0 & 0 & \dots & 0 & 0 & 0 & \dots & 0 & 0 & 0 \\ 0 & 1 & 0 & & 0 & 0 & 0 & & 0 & 0 & 0 \\ 0 & 0 & 1 & \dots & 0 & 0 & 0 & \dots & 0 & 0 & 0 \\ \vdots & & \vdots & & \vdots & & \vdots & & \vdots & & \vdots \\ 0 & 0 & 0 & \dots & 0 & 0 & 0 & \dots & 0 & 0 & 0 \\ 0 & 0 & 0 & & 0 & 0 & 0 & & 0 & 0 & 0 \\ 0 & 0 & 0 & \dots & 0 & 0 & 0 & \dots & 0 & 0 & 0 \\ \vdots & & \vdots & & \vdots & & \vdots & & \vdots & & \vdots \\ 0 & 0 & 0 & \dots & 0 & 0 & 0 & \dots & 1 & 0 & 0 \\ 0 & 0 & 0 & & 0 & 0 & 0 & & 0 & 1 & 0 \\ 0 & 0 & 0 & \dots & 0 & 0 & 0 & \dots & 0 & 0 & 1 \end{bmatrix}$$



Plasma Tomography

- Tomographic inversion

- one reconstruction

$$\mathbf{g} = (\mathbf{P}^T \mathbf{P} + \alpha_1 \mathbf{D}_h^T \mathbf{D}_h + \alpha_2 \mathbf{D}_v^T \mathbf{D}_v + \alpha_3 \mathbf{I}_0^T \mathbf{I}_0)^{-1} \mathbf{P}^T \mathbf{f}$$

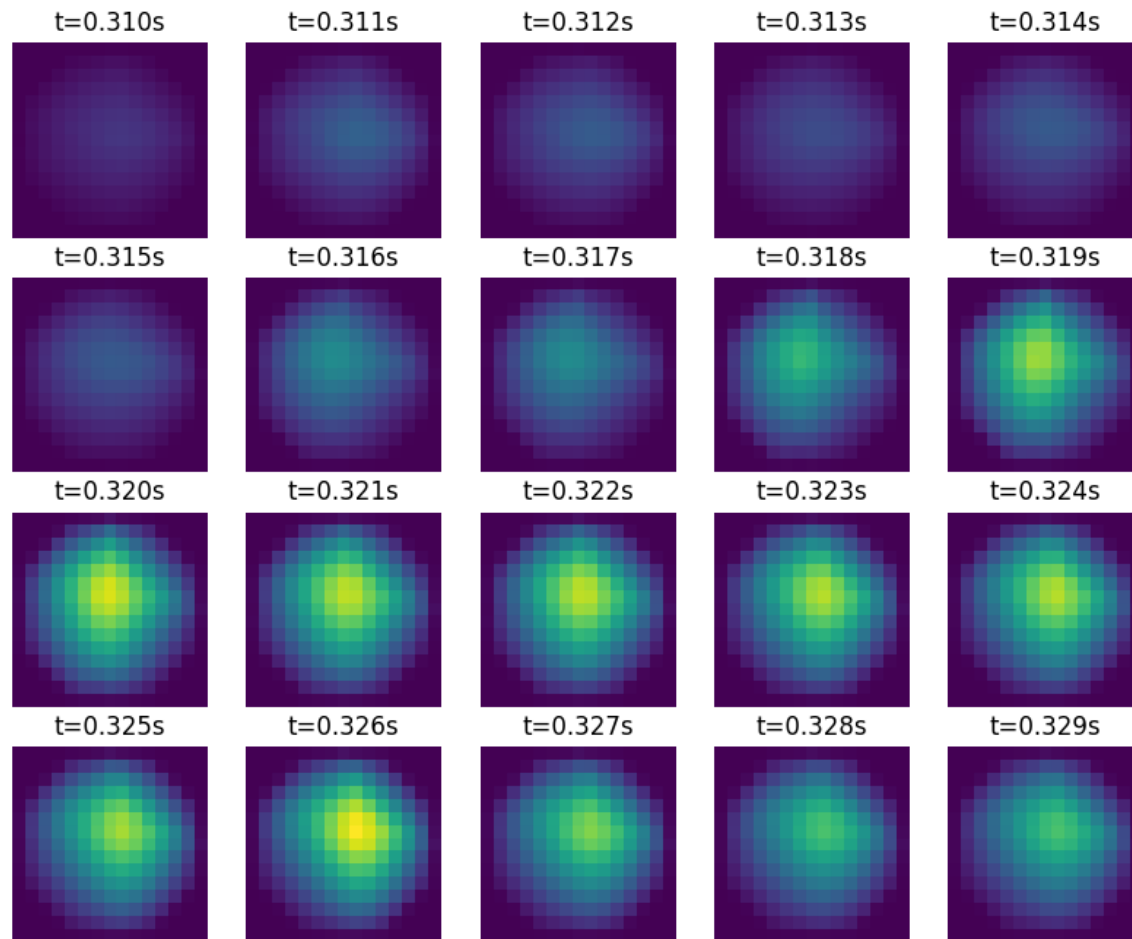
- multiple reconstructions

$$\mathbf{M} = (\mathbf{P}^T \mathbf{P} + \alpha_1 \mathbf{D}_h^T \mathbf{D}_h + \alpha_2 \mathbf{D}_v^T \mathbf{D}_v + \alpha_3 \mathbf{I}_0^T \mathbf{I}_0)^{-1} \mathbf{P}^T$$

$$\mathbf{g} = \mathbf{M} \cdot \mathbf{f}$$

Plasma Tomography

- Tomographic reconstructions for shot 47238



Plasma Tomography

- Source code
 - available at: <https://github.com/diogoff/isttok-tomography>
 - cameras.py
 - finds the lines of sight for a given geometry
 - projections.py
 - finds the projection matrix for a given pixel resolution
 - signals.py
 - reads the camera signals for a given shot number
 - reconstructions.py
 - calculates the reconstructions at given times

Plasma Tomography

- Other forms of regularization
 - generic
 - e.g. minimum Fisher information (MFI)
 - specific
 - e.g. smoothness along magnetic flux surfaces

Plasma Tomography

- Minimum Fisher information (MFI)

$$I_F = \int \frac{g'(x)^2}{g(x)} dx$$

- inspired by the concept of Fisher information
- differences should be small, but they are allowed to be larger where \mathbf{g} itself is large

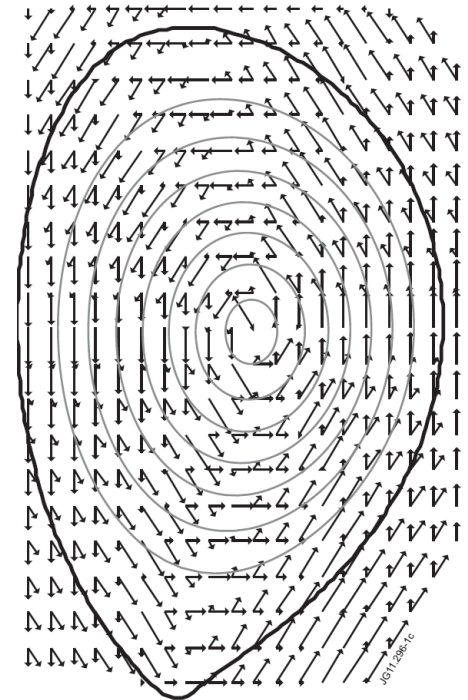
$$\mathbf{g} = (\mathbf{P}^T \mathbf{P} + \alpha_1 \mathbf{D}_h^T \mathbf{D}_h + \alpha_2 \mathbf{D}_v^T \mathbf{D}_v + \alpha_3 \mathbf{I}_0^T \mathbf{I}_0)^{-1} \mathbf{P}^T \mathbf{f}$$

$$\begin{aligned} \mathbf{D}_h^T \mathbf{D}_h &\rightarrow \mathbf{D}_h^T \mathbf{W} \mathbf{D}_h \\ \mathbf{D}_v^T \mathbf{D}_v &\rightarrow \mathbf{D}_v^T \mathbf{W} \mathbf{D}_v \end{aligned} \quad \mathbf{W} = \text{diag} \left(\frac{1}{\mathbf{g}} \right)$$

- system becomes non-linear; solve iteratively for \mathbf{g}

Plasma Tomography

- Smoothness along magnetic flux surfaces
 - differences are taken along the direction of magnetic flux surfaces
 - plasma equilibrium (e.g. by EFIT) must be provided beforehand
 - system remains linear but now depends on data from other diagnostics



$$\mathbf{g} = (\mathbf{P}^T \mathbf{P} + \alpha_1 \mathbf{D}_h^T \mathbf{D}_h + \alpha_2 \mathbf{D}_v^T \mathbf{D}_v + \alpha_3 \mathbf{I}_0^T \mathbf{I}_0)^{-1} \mathbf{P}^T \mathbf{f}$$

Bibliography

- A. C. Kak, M. Slaney, *Principles of Computerized Tomographic Imaging*, SIAM, 2001
- K. McCormick et al., *New bolometry cameras for the JET Enhanced Performance Phase*, Fusion Eng. Des. 74(1-4):679-683, Nov. 2005
- A. Huber et al., *Upgraded bolometer system on JET for improved radiation measurements*, Fusion Eng. Des. 82(5-14):1327-1334, Oct. 2007
- L. C. Ingesson et al., *Soft X ray tomography during ELMs and impurity injection in JET*, Nucl. Fusion 38(11):1675, 1998
- D. R. Ferreira et al., *Full-Pulse Tomographic Reconstruction with Deep Neural Networks*, Fusion Sci. Technol. 74(1-2):47-56, 2018
- P. J. Carvalho, *Tomography algorithms for real-time control in ISTTOK*, PhD thesis, IST/UTL, 2010
- J. Mlynar et al., *Inversion Techniques in the Soft-X-Ray Tomography of Fusion Plasmas: Toward Real-Time Applications*, Fusion Sci. Technol. 58(3):733-741, 2010
- M. Odstrcil et al., *Modern numerical methods for plasma tomography optimization*, Nucl. Instrum. Methods Phys. Res. A 686:156-161, 2012
- V. Loffelmann et al., *Minimum Fisher Tikhonov Regularization Adapted to Real-Time Tomography*, Fusion Sci. Technol. 69(2):505-513, 2016